

# Thermal and chemical pretreatment of *Terminalia mantaly* seed husk biosorbent to enhance the adsorption capacity for $Pb^{2+}$



S.I. Eze, H.O. Abugu\*, O.A. Odewole, N.N. Ukwueze, L.O. Alum

*Department of Pure and Industrial Chemistry, University of Nigeria, Nsukka, Nigeria*

## ARTICLE INFO

### Article history:

Received 13 October 2020

Revised 3 September 2021

Accepted 16 February 2022

Editor: DR B Gyampoh

### Keywords:

Adsorbents

Aqueous solution

$Pb^{2+}$

Isotherm model

*Terminalia mantaly*

Mechanism

## ABSTRACT

A novel biosorbent, modified *Terminalia mantaly* seed (TM) husk was explored for its potential in removing  $Pb^{2+}$  from aqueous solutions. The biosorbent was prepared by pulverizing the husk oven-dried for 1 h at 110 °C. The ground husk was modified at 550 °C and then activated with NaOH and  $H_3PO_4$  to get four different adsorbents. The adsorbents were characterized by Fourier transform Infra-red Spectroscopy (FTIR), Thermogravimetric analyser (TGA), and scanning electron microscope (SEM). The FTIR result showed that there were new functional groups as a result of the activation/modification with heat, NaOH and,  $H_3PO_4$ . The TGA revealed that the modified TM biosorbents were thermally stable up to 400 °C, while the unmodified TM is only thermally stable up to 40–45 °C indicating the differences in the degree of thermal stability. The TGA also revealed that the thermal decomposition of the adsorbents assumed three or less well-pronounced stages, with appreciable mass losses. The SEM image showed that TM possessed the right percentage of carbon content to be used in adsorbent synthesis (> 74%). It also showed that the outer surfaces of the adsorbents were rough and discontinuous in their formation; they cannot be considered as pores but connecting channels to the interior of the adsorbent. Observation revealed that the TM, NaOH and,  $H_3PO_4$  modified TM activated carbon were well described by the Freundlich isotherm model which suggests multilayer  $Pb^{2+}$  binding mechanism onto the adsorbents. Thermally modified *Terminalia mantaly* (TMTM) was experimentally the best adsorbent having the highest adsorption capacity (99.95 mg/g) as predicted by the experimental design result. Performance evaluation of the adsorbents revealed that they are capable of removing  $Pb^{2+}$  ions from aqueous solutions efficiently.

© 2022 The Author(s). Published by Elsevier B.V. on behalf of African Institute of

Mathematical Sciences / Next Einstein Initiative.

This is an open access article under the CC BY license

(<http://creativecommons.org/licenses/by/4.0/>)

## Introduction

The United States Environmental Protection Agency assures us that  $Pb^{2+}$  can affect the nervous system, intelligence, hematopoietic ability, and hearing in children [27]. The chances of contracting cardiovascular diseases increase when the  $Pb^{2+}$  level also increases which may lead to death [16]. With the unceasing development of smelting, electroplating, mining,

\* Corresponding author.

E-mail address: [hillary.abugu@unn.edu.ng](mailto:hillary.abugu@unn.edu.ng) (H.O. Abugu).

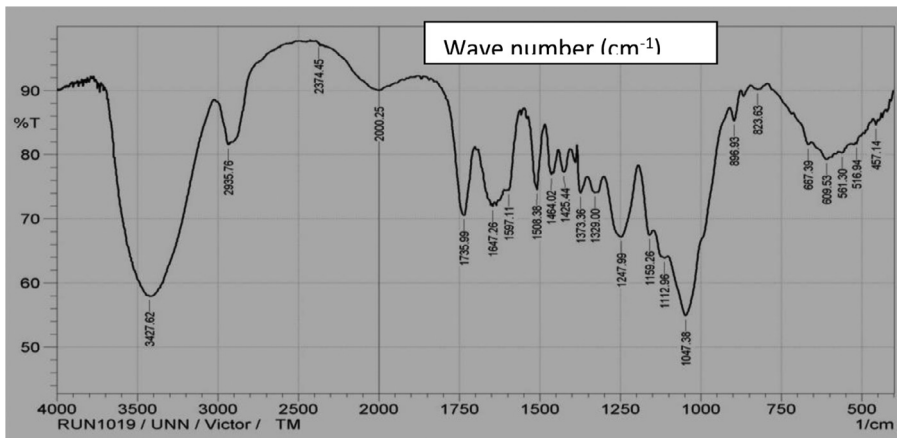


**Fig. 1.** FTIR spectrum of unmodified TM.

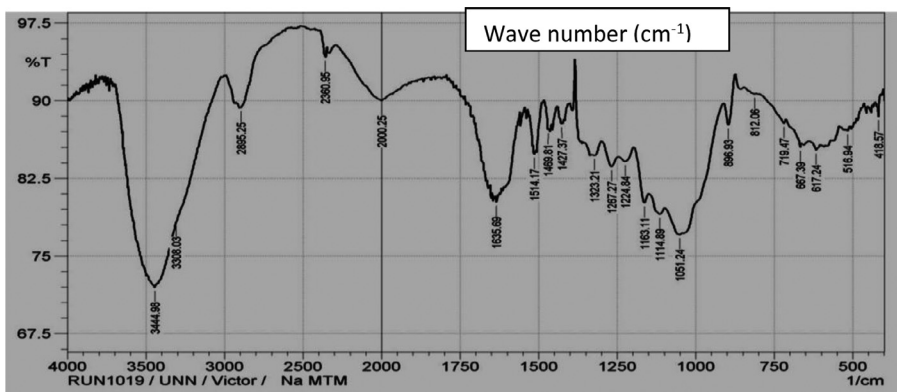


**Fig. 2.** FTIR spectrum of NaOH modified TM.

battery-making, and other industries [28,56], heavy metals including Pb<sup>2+</sup> are released into the water bodies and they are toxic, non-degradable, and often deposited in living tissues [16].

Research has shown several methods for the adsorption of toxic metals from aqueous effluents such as electrochemical or chemical precipitation [13], adsorption on minerals, and reverse osmosis [52–54], ion exchange [10]. With other processes, heavy metal ion adsorption from aqueous solution onto insoluble compounds (adsorbent) is the most effective, cheap, and widely used method [7].

In gas and liquid phases, activated carbons have commonly been used for purification and separation purposes [43,51]. Carbon dioxide, toxic gases, and nitrogen oxides which are particularly toxic constituents of exhaust gases have been removed by adsorption [4,37]. Also in the removal of many inorganic and organic pollutants from liquid phases, like organic dyes and heavy metals, carbon sorbents have been used. Adsorbents of this kind could be derived from many sources such as minerals and lignocellulosic material, though the activated carbon production from minerals has some inherent demerits like low yields, high ash content, and high cost [31,42,45,46]. Alternatively, lignocellulosic materials from agricultural and agro-industrial wastes such as seeds, Bagasse, or peels offer great potential to be applied as precursors considering their high adsorption capacity and proven high carbon content [2,5,6,40].

In recent time, more attention has been shifted to deriving activated carbons from post-industrial and post-agricultural waste materials, like fruit skins and stones, walnut shells, timber production waste *Cassia sieberiana*, Locust bean and Maize husk [14,17,36,50], used car tires, and waste sediments presenting weighty problems to waste management [3,21]. The use of these waste materials for activated carbon production contributes significantly to solving the challenges posed in the management of wastes products. The search for efficient carbonaceous precursor has increased the demand for activated carbon adsorbents.

Notwithstanding the quantum leap in the number of research on the application of plant biomass or wastes as adsorbent around the world, there is no report about the use of sodium hydroxide modified, thermally modified, and unmodified *Terminalia Mantaly* seed as adsorbent. The pyrolysis temperature effect on the porous structure development of the activated carbons, the thermal stability, and their acid-base properties was tested. Here, attempts have been made to produce a novel low-cost adsorbent using *Terminalia Mantaly* seed (TM), an agricultural waste for the removal of Pb<sup>2+</sup> from aqueous solution.

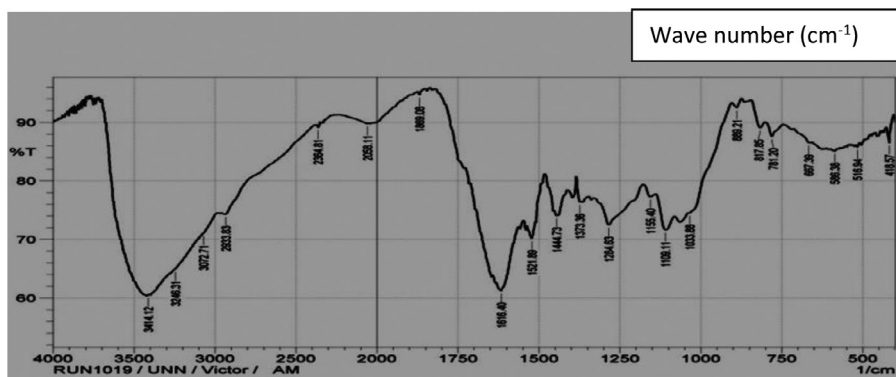
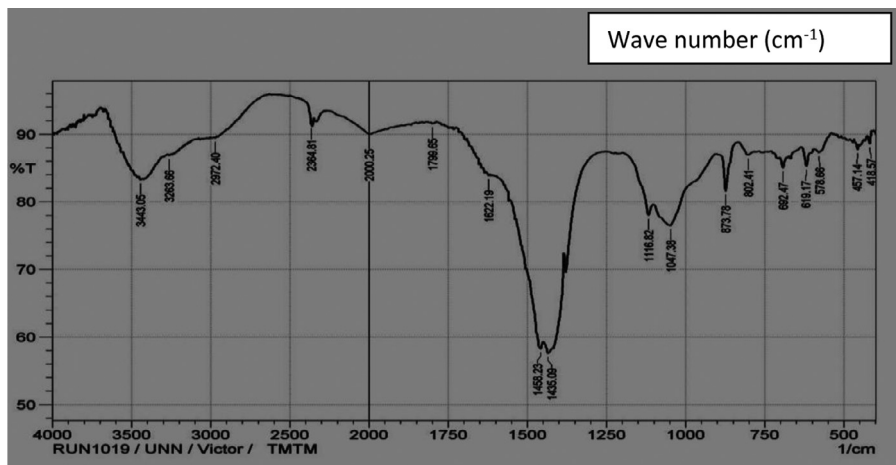
Fig. 3. FTIR spectrum of  $\text{H}_3\text{PO}_4$  modified TM.

Fig. 4. FTIR spectrum of thermally modified TM.

This plant is new in some parts of East and West Africa used mostly for ornamental purposes. *Terminalia Mantaly* seed is present in abundance within the premises of the University of Nigeria Nsukka. The facility maintenance company in the university sees it as a cog in the management of the university's premises.

## Materials and method

### Materials

Sodium hydroxide ( $\text{NaOH}$ ), lead nitrate ( $\text{Pb}(\text{NO}_3)_2$ ),  $\text{H}_3\text{PO}_4$ , Atomic Absorption Spectrophotometer, AAS (Buck scientific model 201, VGP). Fourier transform Infrared spectrophotometer, FTIR, Shimadzu 8400s), Shimadzu Scanning Electron Microscopy (SEM), Thermogravimetric analysis (PerkinElmer TGA).

### Terminalia Manthaly seed husk adsorbent preparation

The *Terminalia Mantaly* (TM) seed husk was identified and classified based on their botanical names by the Taxonomists in the Department of Crop Science, University of Nigeria Nsukka. It was washed with de-ionized water to get rid of undesirable materials. The TM seed was sun-dried for several days, oven-dried at 110 °C for 1 h, and then, ground and pulverized to powdery form which was sieved (125–45  $\mu\text{m}$ ).

50 g of the ground TM seed husk was soaked in 100 mL of 0.5 M  $\text{NaOH}$  for 24 h at room temperature. This was followed by washing severally with deionized water to bring the pH of the washing around neutral. It was then filtered and air-dried to obtain the base modified *Terminalia Mantaly* and stored in an airtight container and finally labeled.

50 g of the ground and sieved (125–300  $\mu\text{m}$  mesh) TM was soaked in 1 M  $\text{H}_3\text{PO}_4$  for 24 h at room temperature. Thereafter, it was washed severally with deionized water to bring the pH of the washing to about 7. It was then filtered, air-dried, and stored in an airtight container which was labeled acid-modified TM. 50 g of the ground TM seed husk was carbonized at 550 °C for 90 min in a muffle furnace, filtered and stored which was also labeled.

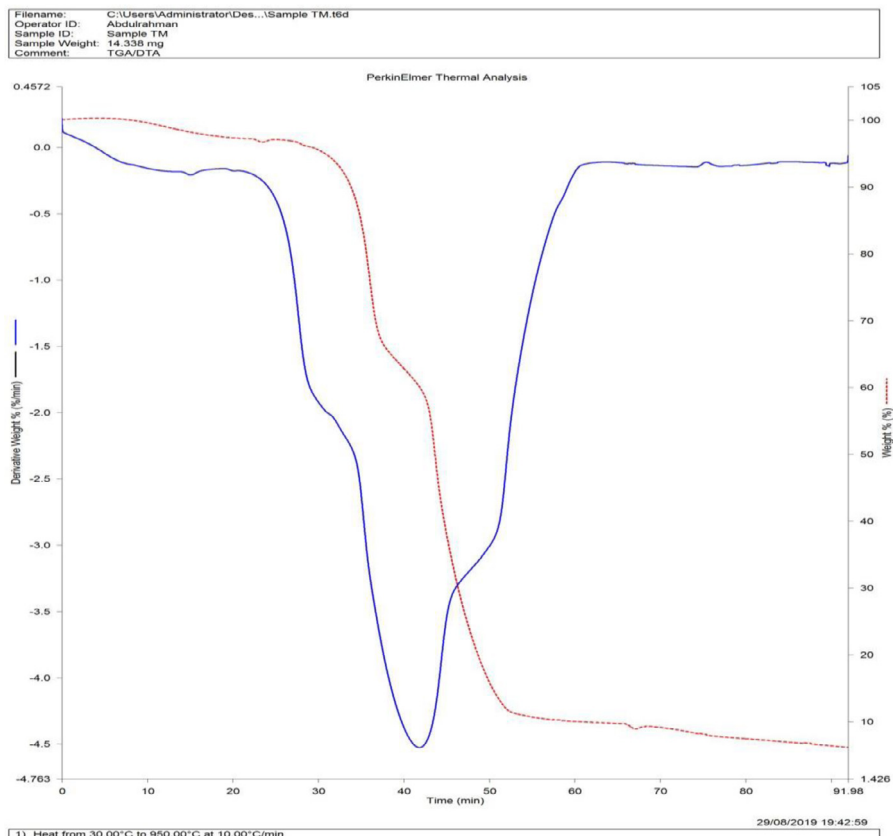


**Fig. 5.** TGA curve for TM.

#### *Adsorbate preparation and adsorption study*

Analytical grade lead nitrate ( $\text{Pb}(\text{NO}_3)_2$ ), was used to prepare 1000 mg/L of  $\text{Pb}^{2+}$  adsorbate using the standard method, from which 200, 400, 600, 800 and, 1000 mg/L were prepared by serial dilution.

Batch adsorption procedure was applied to ascertain the effect of initial metal concentration.

#### *Effects of $\text{Pb}^{2+}$ ion concentration*

0.2 g of the adsorbents were weighed into five different beakers containing 20 mL of 200, 400, 500, 600 and, 800 mg/L  $\text{Pb}^{2+}$ . The beakers were shaken for about 5 min and allowed to stand for 1 h at room temperature. Thereafter, they were filtered and the filtrate was analysed for residual  $\text{Pb}^{2+}$  with AAS. All the adsorbate solution pH was 4.

#### *Calculation of adsorption capacity and percentage removal*

The percentage of lead ions removed and the adsorption capacity of the adsorbent was calculated using Eqs. (1) and (2), respectively.

$$\text{Percentage removal (\%)} = \frac{100(C_0 - C_e)}{C_0} \quad (1)$$

$$q_e \left( \frac{\text{mg}}{\text{g}} \right) = \frac{V(C_0 - C_t)}{m} \quad (2)$$

where  $q_e$  (mg/g) is the adsorption capacity of the adsorbents,  $C_0$  (mg/L) is the initial metal ion concentration in solution,  $C_e$  (mg/L) is the equilibrium ion concentration,  $C_t$  (mg/L) is the metal concentration at time  $t$  in min,  $V$  (liters) is the volume of adsorbate and  $m$  is the mass (g) of the adsorbent.

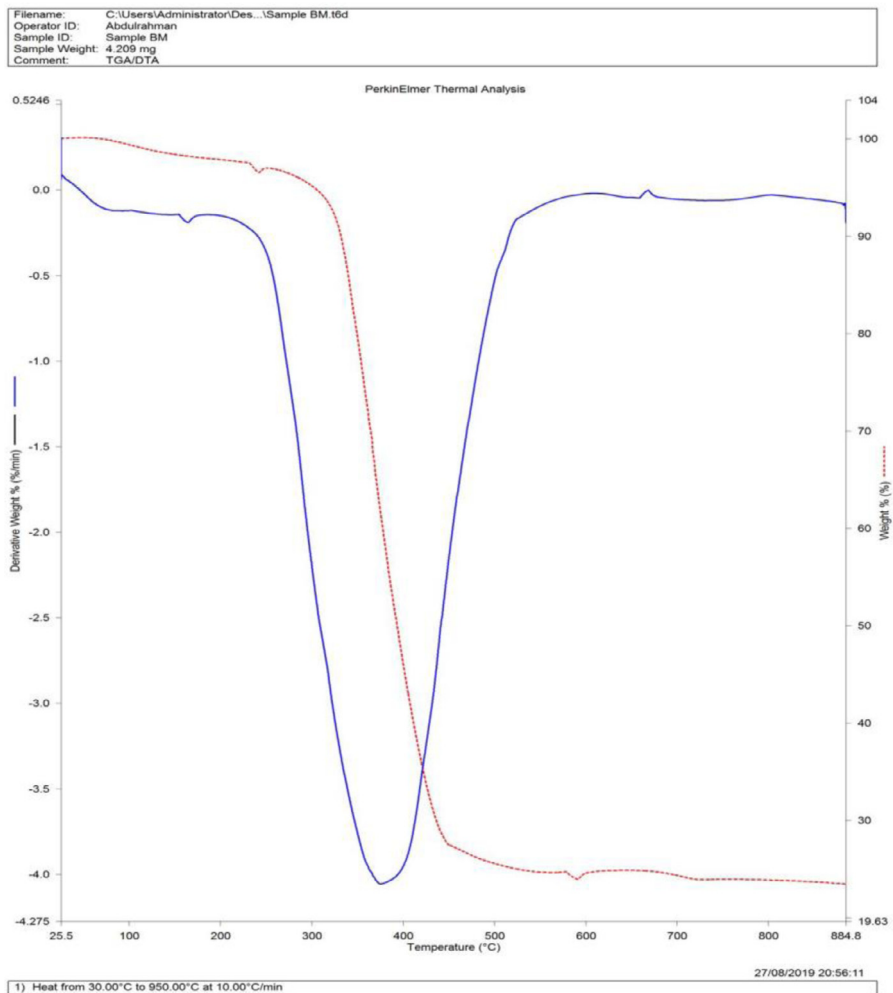


**Fig. 6.** TGA curve for NaMTM.

### Isotherm studies

Batch adsorption technique was used to obtain equilibrium data and it was executed at room temperature and different initial metal concentrations to generate the equilibrium isotherms.

**The Freundlich isotherm model** suggests heterogeneous surface energies and it presents the exponential distribution of active sites available in the adsorbent [22]. The model equation was applied to give the relationship between the amount of adsorbate sorbed by the adsorbent and the metal in solution. The model equation in linear form is:

$$\log q_e = \log K_f + \frac{1}{n} \log C_e \quad (3)$$

where  $q_e$  is the amount of  $\text{Pb}^{2+}$  sorbed (mg/g),  $C_e$  is the equilibrium concentration of the  $\text{Pb}^{2+}$ .  $K_f$  and  $n$  are the Freundlich constants which represent the adsorption capacity and the adsorption intensity of the activated carbon (AC) [25,49].  $K_f$  and  $n$  are estimated from the slope and intercept of  $\log q_e$  versus  $\log C_e$  plot.

**The Langmuir Adsorption Isotherm model** describes quantitatively the formation of monolayer adsorbate on the outer surface of the adsorbent. It is represented as

$$\frac{C_e}{q_e} = \frac{1}{Q^o b} + \frac{C_e}{Q^o} \quad (4)$$

Where  $C_e$  is the equilibrium concentration of adsorbate (mg/L),  $q_e$  is the amount of metal adsorbed per gram of the adsorbent at equilibrium (mg/g),  $Q^o$  is the maximum monolayer coverage capacity (mg/g) and  $b$  is the Langmuir isotherm constant (L/mg).  $Q^o$  and  $b$  were calculated from the slope and intercept of the linear Langmuir plot of  $C_e/q_e$  versus  $C_e$ . The

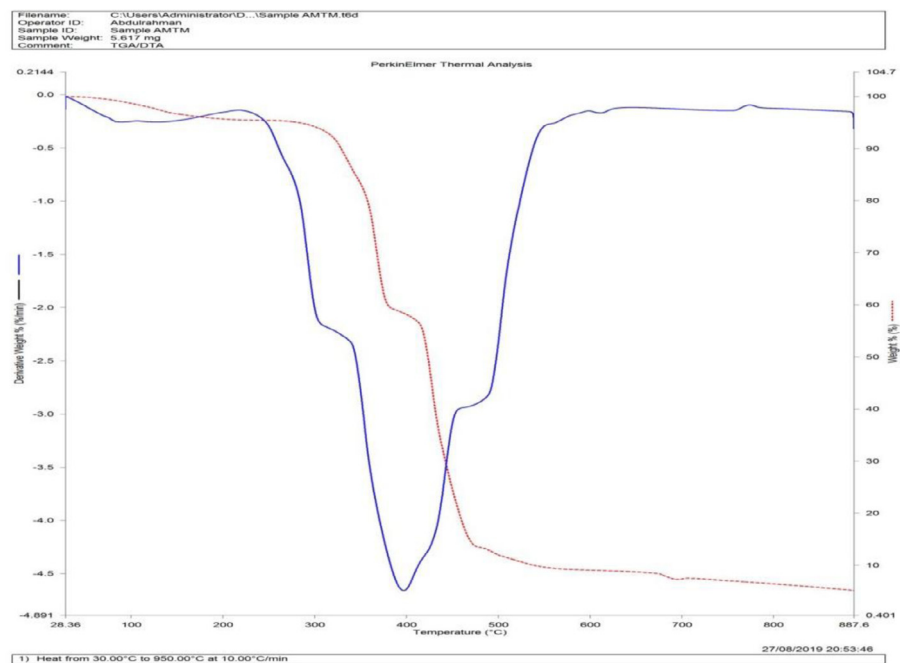


Fig. 7. TGA curve for AMTM.

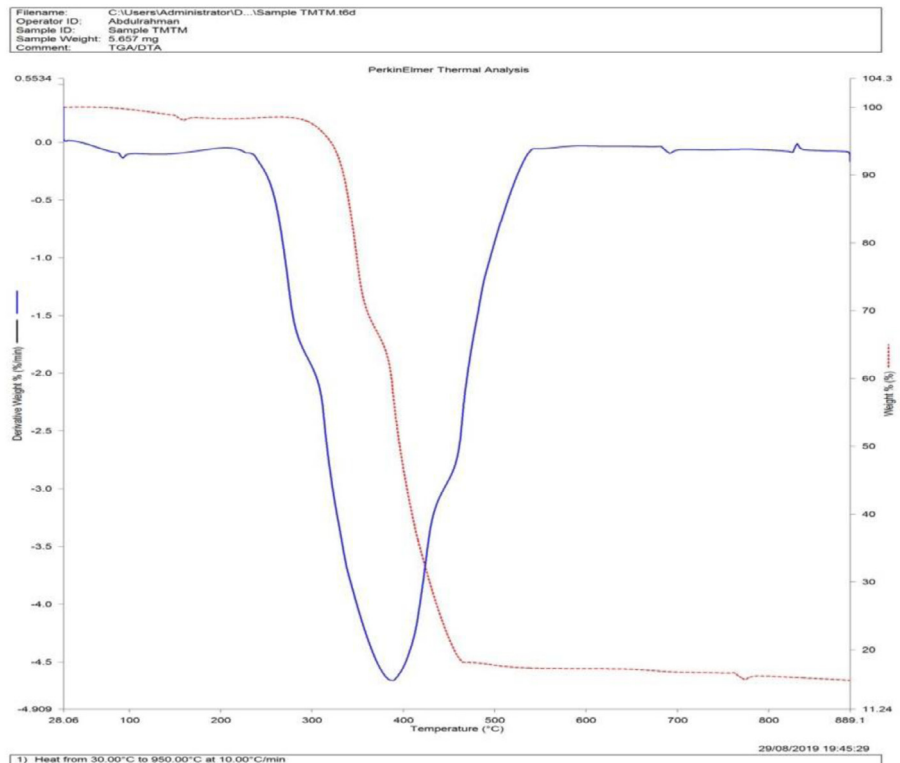


Fig. 8. TGA curve for TMTM.

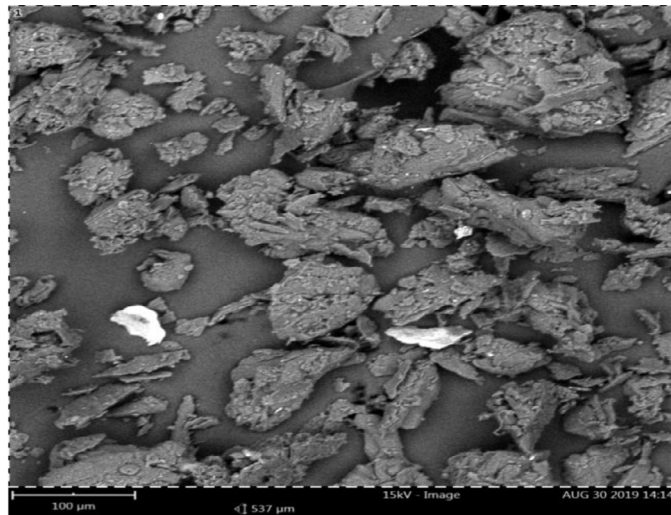
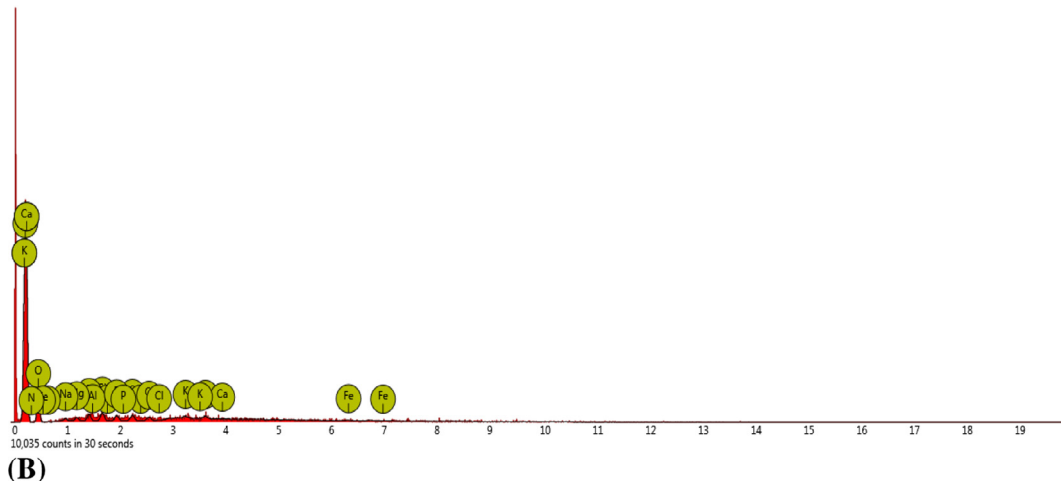
(A)FOV: 537  $\mu\text{m}$ , 15kV Mode image, BSD full Detector, Time: AUG 30 2019 14:14

Fig. 9. SEMImage and elemental content of unmodified TM.

affinity between the adsorbent and adsorbate using the dimensionless separation factor  $R_L$  was estimated using Langmuir isotherm parameter b in  $R_L = 1/(1+bCo)$ , where Co is the initial metal concentration.

**Temkin isotherm model** is a case that ignores the extremely low and large adsorbate concentration values while taking account of adsorbent-adsorbate interactions. The model assumes a linear decrease in the heat of adsorption of all molecules in the layer, rather than logarithmic with coverage [8,48].

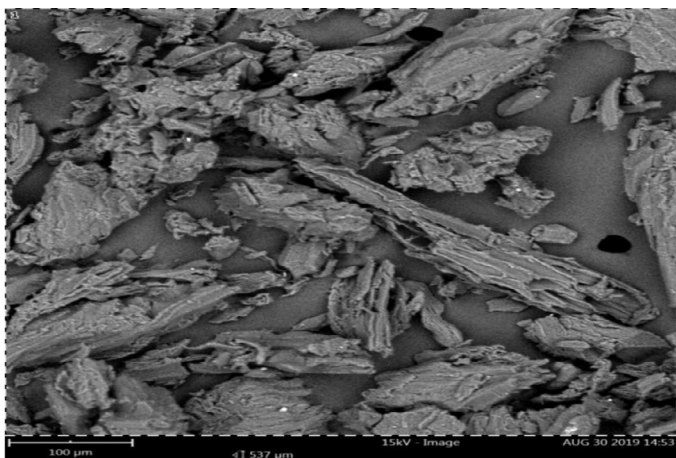
*It is represented as*

$$q_e = B_T \ln A_T + B_T \ln C_e \quad (5)$$

Where  $B_T = RT/b_T$ , R is the universal gas constant (8.314 J/mol/K),  $b_T$  is Temkin isotherm constant related to the heat of sorption (J/mol), T is the temperature (298 K),  $A_T$  is Temkin isotherm equilibrium binding constant (L/mg). The constants were estimated from the slope and intercept of  $q_e$  against  $\ln C_e$  plot.

**Dubinin Radushkevich isotherm model** (D-R) is generally applied to express the adsorption mechanism with Gaussian energy distribution onto a heterogeneous surface [12,18]. The model is expressed as

$$\ln q_e = \ln(q_s) - (K_{ad} \epsilon^2) \quad (6)$$



(A)FOV: 537  $\mu\text{m}$ , 15kV Mode image, BSD full Detector, Time: AUG 30 2019 14:53

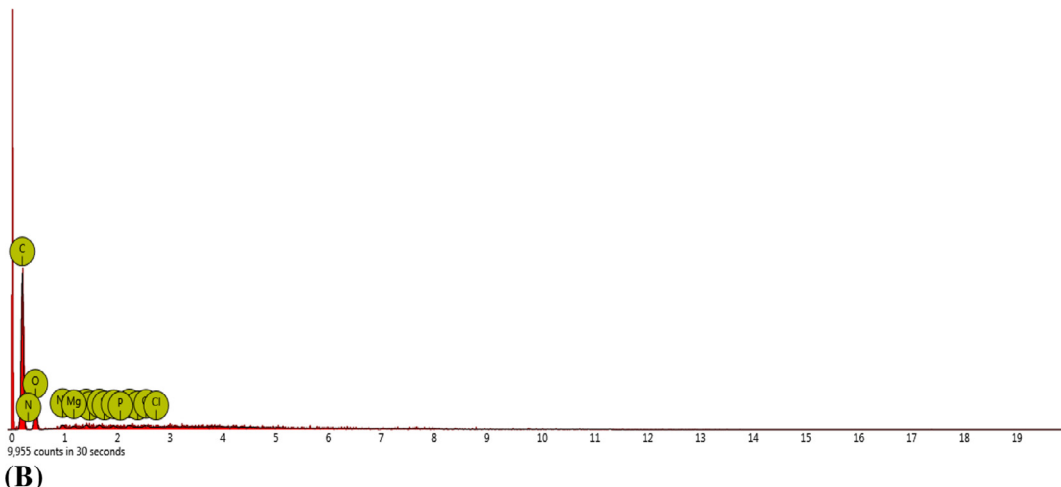


**Fig. 10.** SEM image and elemental content of NaOH modified TM.

Where  $q_e$ , is the amount of adsorbate in the adsorbent at equilibrium (mg/g),  $q_s$ , is the theoretical isotherm saturation capacity (mg/g),  $K_{ad}$  is the Dubini-Radushkevich isotherm constant relating to the adsorption energy ( $\text{mol}^2/\text{kJ}^2$ ) and  $\varepsilon$  is the Dubinin-Radushkevich isotherm constant which is given as  $R\ln[1+1/C_e]$ . The constants are calculated from the plot of  $\ln q_e$  against  $\varepsilon^2$ .

The information about the physicochemical characteristic of the adsorption process is provided by the sorption energy  $E$  or mean free energy (kJ/mol). When the  $E$  value falls between 8 and 16 kJ/mol, then the adsorption occurred via a chemical ion-exchange process, else ( $E$  less than 8 kJ/mol), the sorption process is of physical nature [15]. The mean free energy  $E$  is given as

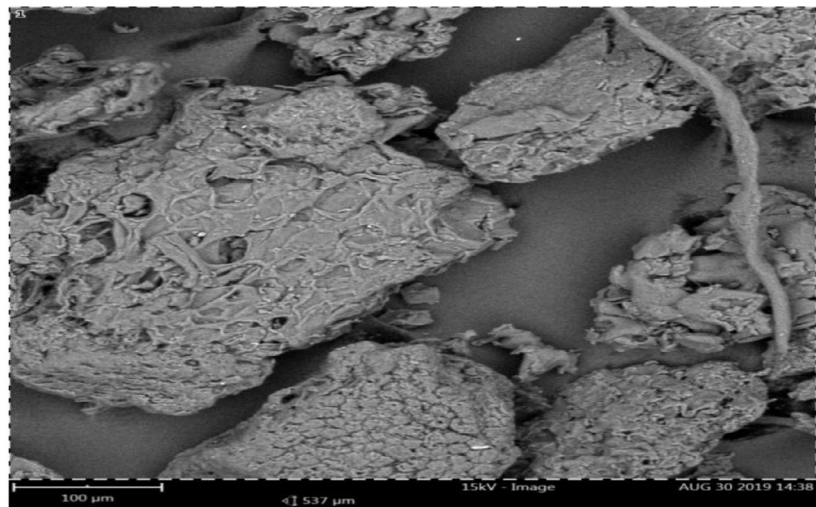
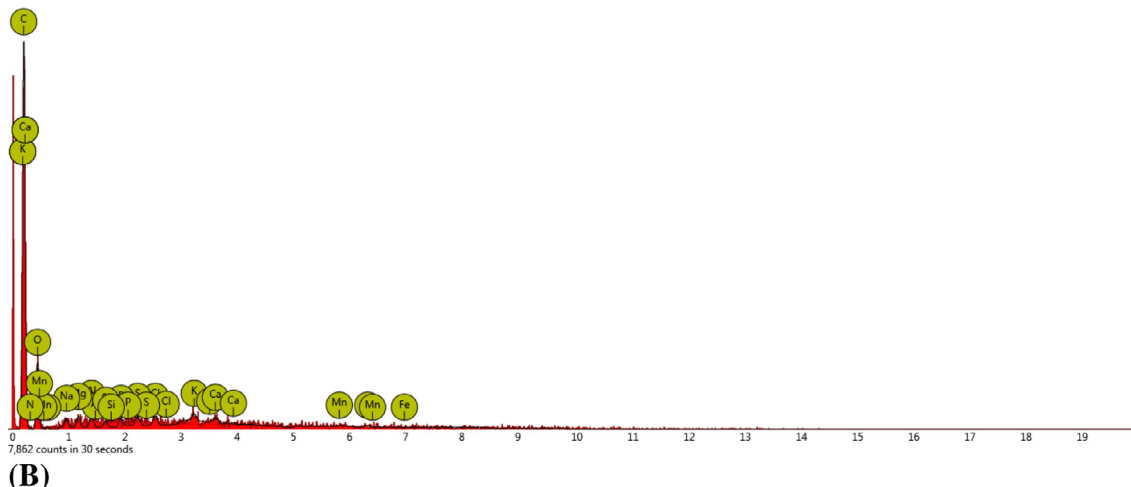
$$E = 1/\sqrt{2K_{ad}} \quad (7)$$

#### Experimental design

Before the laboratory work, the optimal (custom) design method was applied using design expert version 11 software to predict the best adsorbate concentration at which maximum adsorption capacity can be achieved.

#### Statistical analysis

The data are listed as mean  $\pm$  standard error of the mean since the study was carried out in triplicate.

(A)FOV: 537  $\mu\text{m}$ , 15kV Mode image, BSD full Detector, Time: AUG 30 2019 14:38

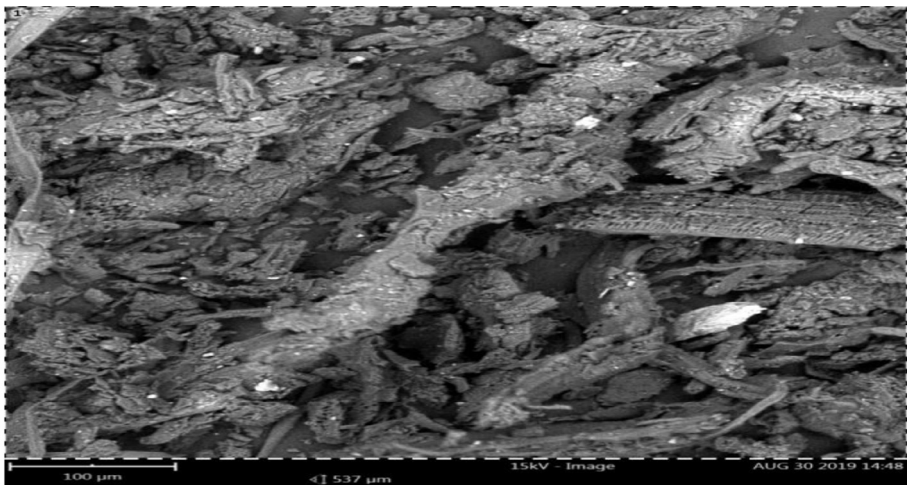
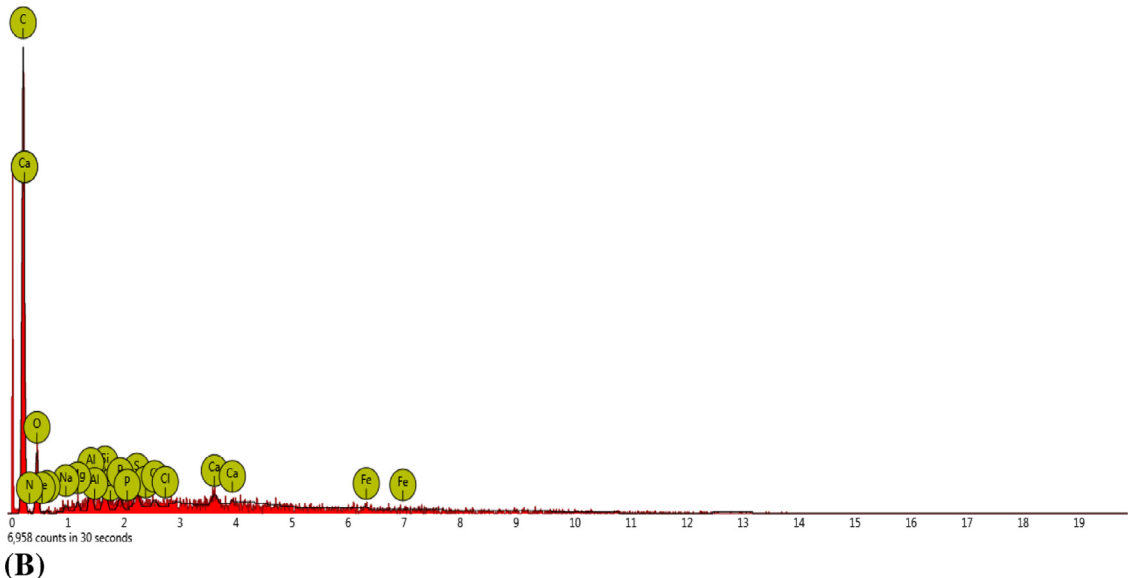
(B)

Fig. 11. SEM image and elemental content of thermally modified TM.

## Results and discussion

The types of functional groups present on the surface of the carbon enable the comprehension of the adsorption mechanism of ionic adsorbate on activated carbons [35]. The presence of a functional group on the surface of activated carbon influences the adsorption capacity. They affect the adsorption behavior as well as dominate the adsorption mechanism. Functional groups tend to reduce the binding energy while increasing the uptake kinetics at a monolayer coverage [57].

The FTIR results of the unmodified TM, base (NaOH) modified, acid ( $\text{H}_3\text{PO}_4$ ) modified and thermally modified *Terminalia Mantaly* seed husk (Figs. 1–4) spectra, showed the presence of carboxyl, hydroxyl and, carbonyl functional groups in the range 2935.76, 3427.62 and 1047  $\text{cm}^{-1}$ , respectively. Generally, the stretching vibrations due to N-H groups overlapped by the absorption bands of hydroxyl groups appeared within the range of 3427.62  $\text{cm}^{-1}$  [14]. The band of minor intensity which appeared at 2935.76  $\text{cm}^{-1}$  corresponds to the asymmetric stretching vibrations of alkyl chains whereas that of medium intensity at 1647.26 and 1597.11  $\text{cm}^{-1}$  appeared due to C = O stretching vibrations. It can be observed that after acid and thermal modification, the absorption bands appeared at similar positions with less intensity. The OH and carboxyl groups stretching vibrations appeared at 3416.06 and 3443.06  $\text{cm}^{-1}$  and medium intensity appeared at 1635.69 and 1622.19  $\text{cm}^{-1}$  showing the C = O stretching vibration. The changes in the band at 3416.06 and 3443.06  $\text{cm}^{-1}$  were observed, showing that acid and thermal treatment had a significant effect on both the functional groups. The presence of the hydroxyl and carboxyl groups on the surface of both the unmodified and modified biosorbent enhances the adsorptive capacity and the banding of positively charged cations on the surface of the adsorbent according to [24].

(A) FOV: 537  $\mu\text{m}$ , 15kV Mode image, BSD full Detector, Time: AUG 30 2019 14:48Fig. 12. SEM image and elemental content of  $\text{H}_3\text{PO}_4$  modified TM.

The interaction of heteroatom (oxygen, nitrogen, sulphur) from within the precursor and from the atmosphere and free radicals on the carbon surface during activation leads to the formation of functional groups [14,55]. The functional groups make the activated carbon surface to be reactive chemically and enhance its adsorptive ability [30]. The oxidation of the activated carbon surface is an inherent characteristic in activated carbon production. It results in the formation of carbonyl (=CO), carboxylic (-COOH), and hydroxyl (-OH), groups imparting an amphoteric feature to the activated carbon. So it can be either basic or acidic which contributes more to the interaction between  $\text{Pb}^{2+}$  and the surface of the adsorbents.

The TGA analysis (Figs. 5–8) showed that AMTM, NaMTM and, TMTM are thermally stable up to 400 °C, while unmodified TM is only thermally stable at 40–45 °C indicating the differences in the degree of thermal stability. The TGA curves of the thermal decomposition of all the adsorbent types under consideration took place in three or less well-pronounced stages, with appreciable mass losses, but the loss of mass accompanying them were quite dissimilar and took place in temperatures of many slim ranges. The initial mass loss from 0 to 200 °C (0 to about 20 min), is attributed to the adsorbed moisture since the TM husk was hitherto dried at about 110 °C for 1 h. The second mass loss step from 200 to 350 °C (about 20 to 35 min) is ascribed to the thermal degradation of hemicellulose and cellulose, forming a carbonaceous residue from 350 °C which decomposes slowly up to 400 °C. The end product residue formed was about 10%, which is coherent with a mixture of ash and carbon. Similar results were observed by Oliveira et al [39], in the TGA/DTA analysis of renewable biomass, Babassu and Bazan et al [9], in the thermal analysis of activated carbon secured from remnants of supercritical extraction of hops.

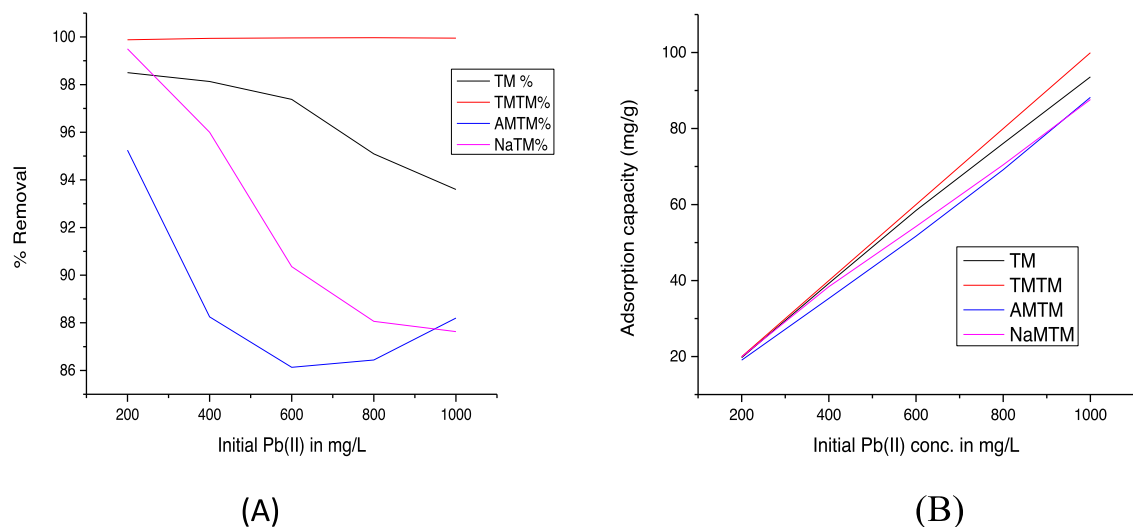


**Fig. 13.** Effect of initial concentration on the percentage removal (A) and the adsorption capacity (B) of Pb(II) by TM, TMTM, AMTM and NaMTM.

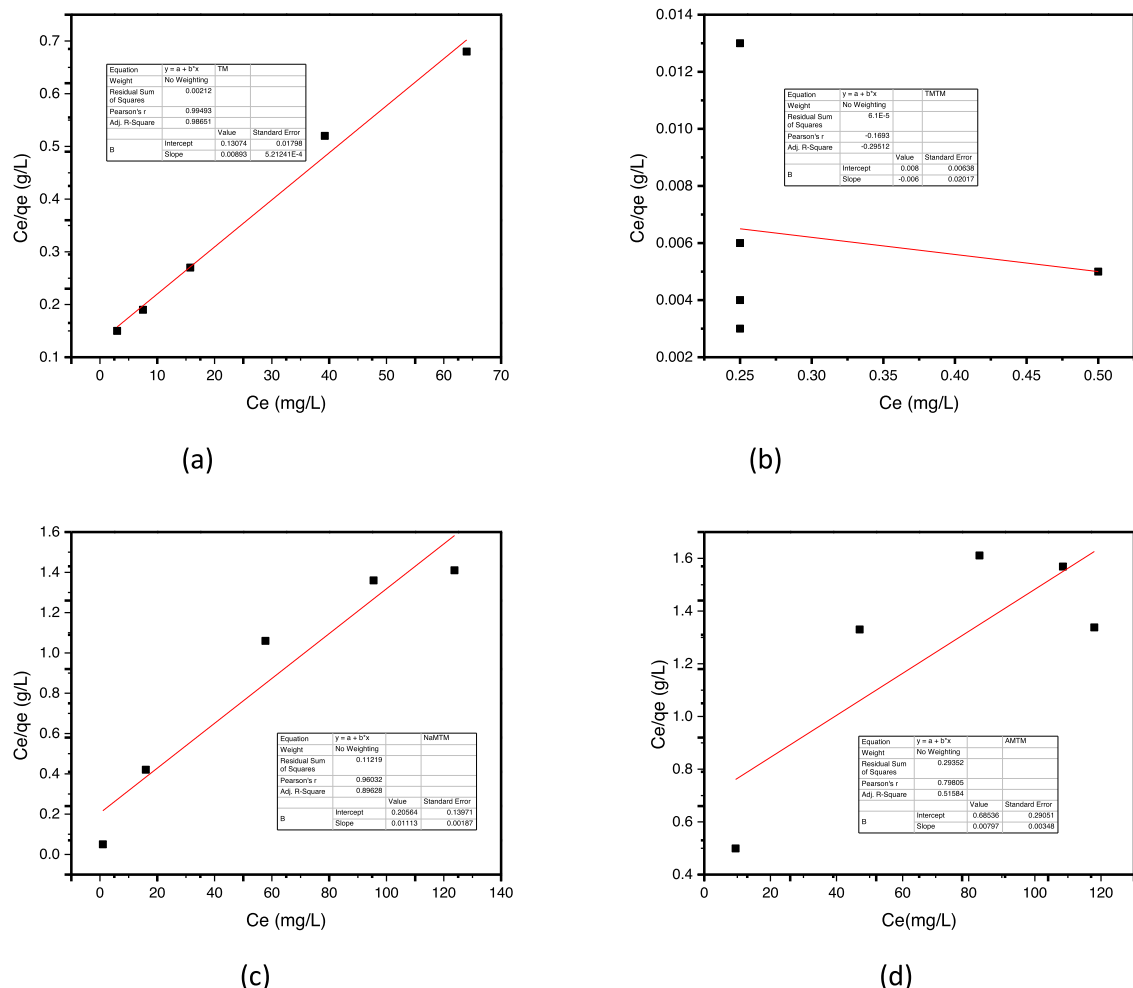


**Fig. 14.** Langmuir isotherm plot for adsorption of Pb<sup>2+</sup> ion by TM(a), TMTM(b), NaMTM(c) and AMTM(d).

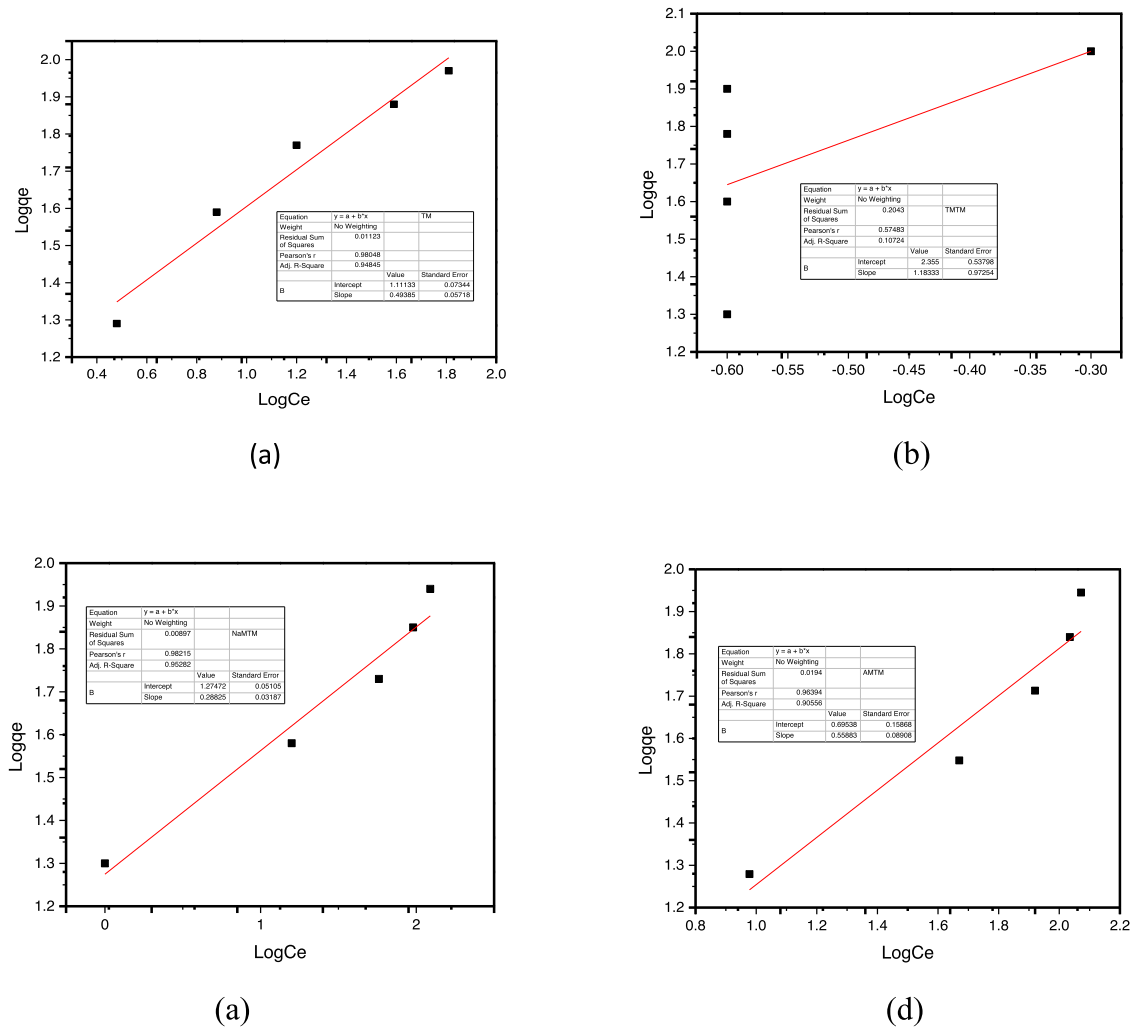


**Fig. 15.** Freundlich isotherm plot for adsorption of Pb(II) ion by TM(a), TMTM(b), NaMTM(c) and AMTM(d).

Presented in Fig. 9 through 12 are the morphological characteristics obtained from scanning electron microscope images and their respective elemental content for the TM, NaMTM, TMTM and, the AMTM. It could be observed that TM is a potential adsorbent owing to the percentage carbon contents, the most important feature of an adsorbent precursor which was in the neighborhood of 74–80%. The surface topology of the TM is different from the modified TM indicating the need for modification. The modified TM showed rough surface area, unlike the unmodified TM which had a smooth surface indicating lower pores on the surface of the adsorbent. The SEM image showed the outer surfaces of the adsorbents were rough and discontinuous in their formation; they cannot be considered as pores but connecting channels to the interior of the adsorbent. The surface area of the modified TM improved due to the oxidizing effect of the modifying agent which in turn, enhances the adsorption capacity of the adsorbents. The presence of heteroatom on the adsorbents surface, during activation helps the formation of functional groups by the interaction of atoms such as O<sub>2</sub> and N<sub>2</sub>, (both from the atmosphere and within the precursor) with free radicals on the carbon surface [47,55]. Also, it was observed that the carbon content of the modified TM (NaMTM, TMTM and, the AMTM) decreased as a result of the burn-off emanating from the oxidizing effect of the modifying agent on the TM.

The adsorption rate of metal ion onto adsorbents is a function of the initial metal concentration which makes it an important parameter to be considered in assessing the effectiveness of adsorbents. Observation showed that the percentage removal of the Pb<sup>2+</sup> (Fig. 13A), decreased with an increase in the initial metal ion concentration from 200 to 1000 mg/L and after which, it became relatively stable. The reduction in adsorption is due to adsorbents having a fixed number of adsorptive sites (as stated by Langmuir isotherm model), which at higher concentrations, the active sites become saturated [11]. On the other hand, an increase in the adsorption capacity for Pb<sup>2+</sup> with an increase in the initial metal ion concentration was observed (Fig. 13B). This is ascribed to the concentration gradient increase which is the driving force to surmount the

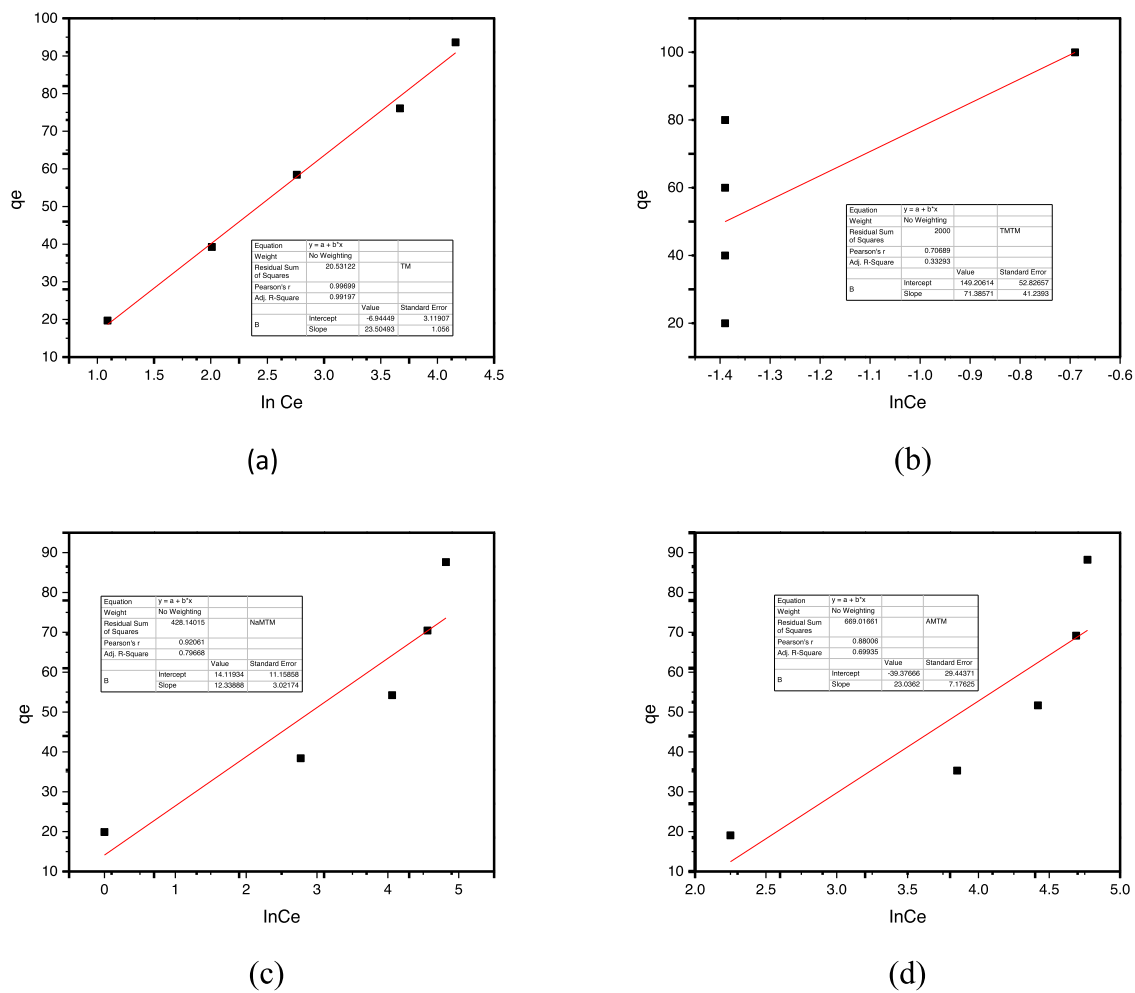


**Fig. 16.** Temkin isotherm plot for adsorption of Pb(II) ion by TM(a), TMTM(b), NaMTM(c) and AMTM(d).

resistance to mass transfer of the  $\text{Pb}^{2+}$  between the adsorbent species and adsorbate which is in line with the observation of.

An adsorption isotherm expresses the relationship among the measure of solute taken-up and the measure of solute in the solution phase. Since adsorption isotherm is essential to describing how adsorbent interacts with the adsorbate therefore, it is very essential for the scheming of new adsorbents. Freundlich, Langmuir, Temkin and D-R Isotherm models were applied to determine the sorption parameters and, identify the model that best explains the adsorption processes by these prepared adsorbents. The experimental data obtained were fitted into the linear equation of the isotherm models (Figs. 14–17), and their adsorption capacities were calculated. The values of  $q_e$  and  $K_L$  for Langmuir,  $K_f$  and,  $n$  for Freundlich and  $B_T$  and  $A_T$  for Temkin isotherm are listed in Table 3 with their respective determination coefficient ( $R^2$ ). The Langmuir isotherm model suggests that sorption occurs on a homogeneous surface by monolayer sorption without interaction between sorbed ions.

$Q_L$  (adsorption capacity) and  $K_L$  (energy of adsorption) are the Langmuir isotherm constants (Uddin, 2007), and  $R_L$  (separation factor) values indicates the adsorption irreversibility ( $R_L = 0$ ), unfavorable ( $R_L \geq 1$ ) or favorable ( $R_L > 0$  and  $R_L < 1$ ) Table 1. presents the calculated  $R_L$  values and it could be established that the affinity between the adsorbent and adsorbate was favorable in all the adsorbents type except in TMTM were it was negative. This could be attributed to the electrostatic nature of the adsorption process. Notwithstanding, such negative values are not usually observed, but it has been reported previously [20,26,38], also observed negative values of the Langmuir constants and noted that it was as a result of bad linearization. The observed  $R_L$  values decreased as the initial metal ion was increased showing  $\text{Pb}^{2+}$  uptake was favorable. Mustapha et al [34]. observed a similar result from the adsorption of  $\text{Pb}^{2+}$ ,  $\text{Cd}^{2+}$ ,  $\text{Zn}^{2+}$  and,  $\text{Cu}^{2+}$  using *Albizia lebbeck* pods.

The Freundlich model, which gives an exponential distribution of active sites existing in the activated carbon (AC), predicts heterogeneous surface energies. The Freundlich constants ( $K_f$  and  $n$ ) indicate the adsorption capacity and adsorption intensity of the adsorbent, respectively [25,49]. When  $n > 1$ , the adsorption coefficient increases with an increase in the con-

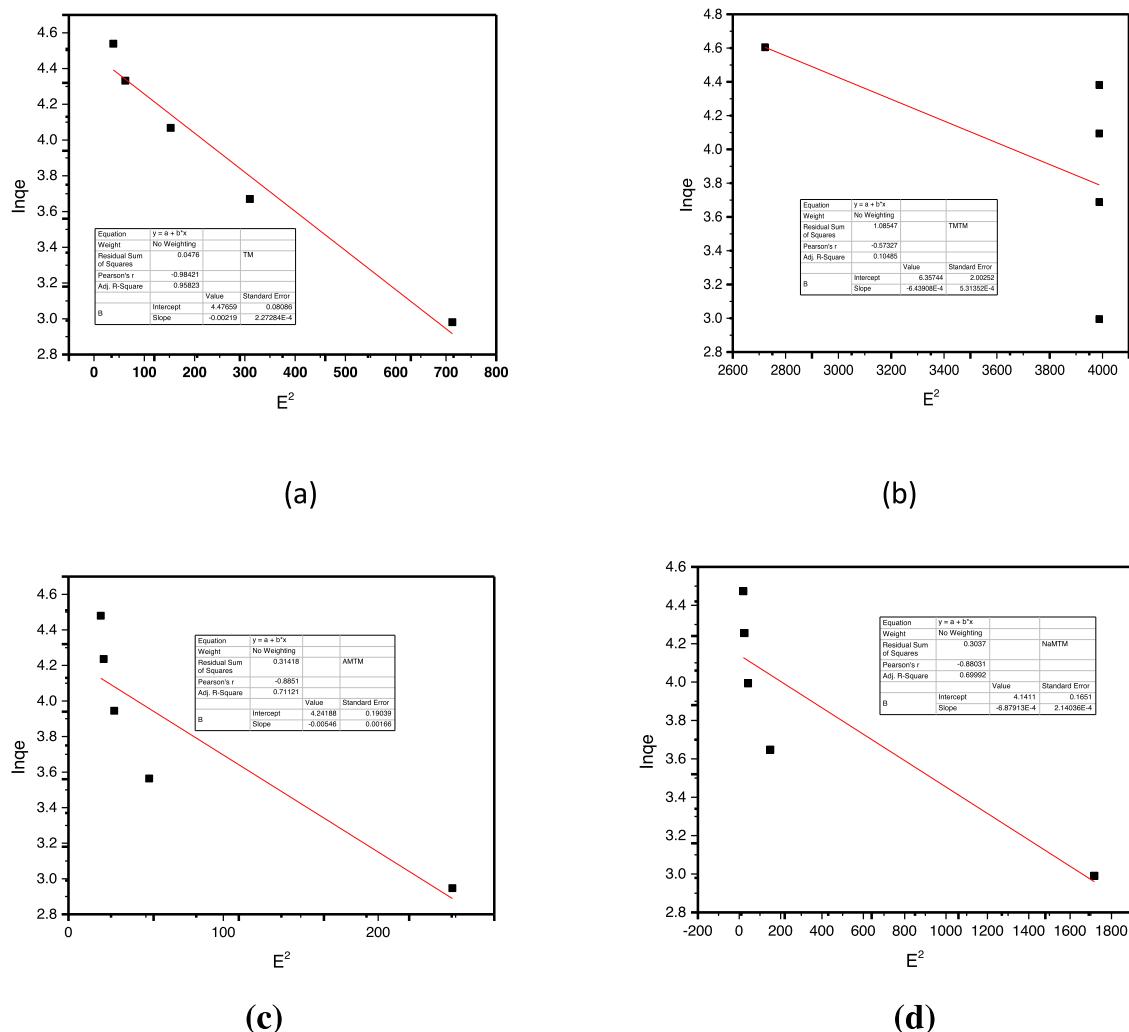


**Fig. 17.** Dubinin radushkevich isotherm plot for adsorption of  $\text{Pb}(\text{II})$  ion by TM(a), TMTM(b), AMTM (c) and NaMTM (d).

**Table 1**  
Separation factor  $R_L$  for  $\text{Pb}^{2+}$  removal.

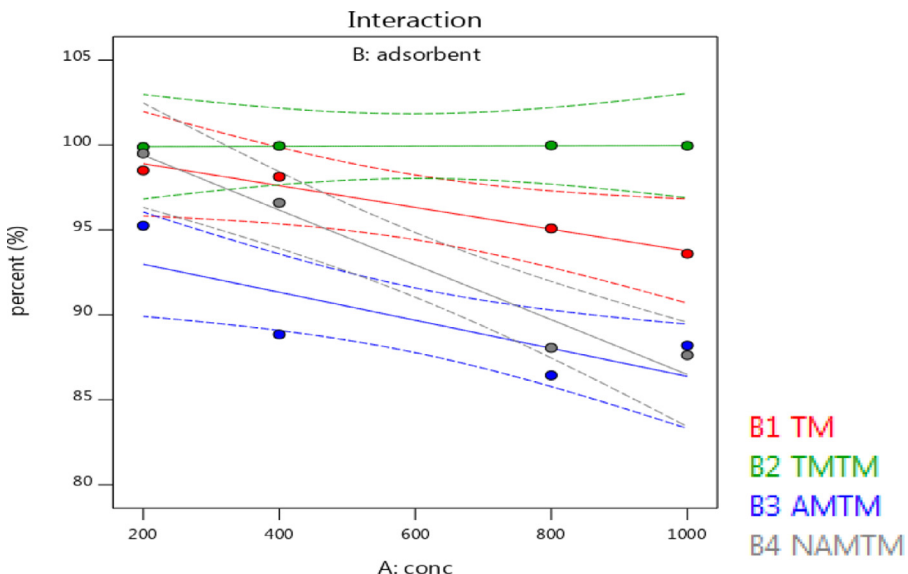
Initial $\text{Pb}^{2+}$ concentration	AMTM	TM	TMTM	NaMTM
200	0.294118	0.068493	-0.00067	0.047619
400	0.172414	0.035461	-0.00033	0.02439
600	0.121951	0.023923	-0.00022	0.016393
800	0.09434	0.018051	-0.00017	0.012346
1000	0.076923	0.014493	-0.00013	0.009901

**Table 2**  
The adsorption capacity (mg/g) and percentage removal by the biosorbents.

TM $q_e$	TMTM $q_e$	AMTM $q_e$	NaMTM $q_e$	TM (%)	TMTM (%)	AMTM (%)	NaMTM (%)
19.70	19.98	19.05	19.90	98.5	99.88	95.25	99.50
39.25	39.98	35.3	38.40	98.13	99.94	88.25	96.00
58.43	59.98	51.68	54.23	97.38	99.96	86.13	90.36
76.08	79.98	69.15	70.45	95.09	99.97	86.44	88.06
93.6	99.95	88.2	93.60	99.95	88.2	88.2	87.63

**Table 3**  
Isotherm model parameters.

Isotherm Model	AMTM	TM	TMTM	NaMTM
<b>Langmuir</b>				
$Q^o$ (mg/g)	125 ± 0.020	112.4 ± 0.231	-16.67 ± 0.042	90.09 ± 0.310
b (L/mg)	0.012 ± 0.000	0.068 ± 0.001	-7.49 ± 0.011	0.05 ± 0.026
$R^2$	0.515	0.987	-0.295	0.896
<b>Freundlich</b>				
$K_F$ (mg/g)	4.95 ± 0.593	12.92 ± 0.753	226.46 ± 0.959	18.82 ± 1.022
n	1.787 ± 0.239	2.03 ± 0.110	0.85 ± 0.090	3.47 ± 0.081
$R^2$	0.906	0.948	0.107	0.953
<b>Temkin</b>				
$B_T$	23.04 ± 0.360	23.505 ± 0.021	71.386 ± 0.471	12.34 ± 0.651
$A_T$ (L/g)	0.181 ± 0.542	0.752 ± 0.001	8.087 ± 0.832	3.14 ± 0.222
$R^2$	0.699	0.992	0.332	0.797
<b>Dubini-R</b>				
$q_s$ (mg/g)	69.53	97.93	572.49	62.87
$K_{ad}$ (mol <sup>2</sup> /kJ <sup>2</sup> )	5.46E-3	2.19E-3	6.43E-4	6.88E-4
$R^2$	0.797	0.997	0.333	0.699
E	9.569	15.110	777.508	726.850

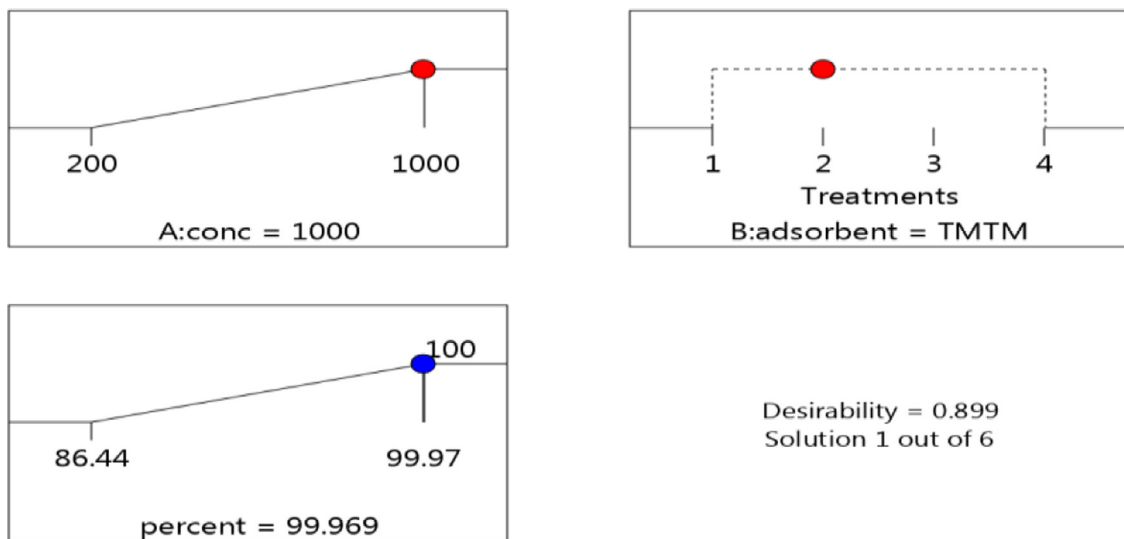


**Fig. 18.** Adsorbent-adsorbate concentration interaction.

centration of the solution leading to an increase in hydrophobic surface characteristic after monolapsian, and when  $n < 1$ ,  $K_f$  decreases with concentration [19]. The obtained  $n$  value was all greater than unity except for TMTM ( $n = 0.85$ ) adsorbent indicating an increase in adsorption as the  $Pb^{2+}$  concentration increased. It was also observed for TMTM in Langmuir model that it had negative (-7.49 L/mg) energy of adsorption.

Temkin isotherm model presumes heat of adsorption (a function of temperature) of all molecules in the layer of adsorbent would linearly decrease, rather than logarithmic with coverage [8], due to adsorbent-adsorbate interactions, and that the adsorption is characterized by a uniform distribution of the binding energies, up to some maximum binding energy.  $A_T$  is the equilibrium binding constant which corresponds to the maximum binding energy,  $B_T$  is related to the heat of adsorption. From the assessment of the fitness of the data onto the isotherm models, it could be observed that TM, AMTM and, NaMTM with  $R^2$  of 0.948, 0.906 and, 0.953, respectively, are best fitted into the Freundlich isotherm model (Table 3), while none of these isotherm models could satisfactorily explain the adsorption processes in TMTM considering their  $R^2$  values though, Temkin isotherm model could be likened to the explanation of the adsorption process of  $Pb^{2+}$  onto TMTM having had the best  $R^2$  (0.332).

The application of Dubinin Radushkevich model gave adsorption energies 9.569, 15.110, 777.508 and 726.850 kJ/mol for AMTM, TM, TMTM and NaMTM at 298 K, respectively. This suggests that the adsorption of  $Pb^{2+}$  on these adsorbents involved multilayer nature, which includes Van Der Waals forces since the free energy E, were  $> 8$  kJ/mol suggesting chemical adsorption. The monolayer adsorption stage, ion-exchange and, Van Der Waals interactions were predominantly implicated

**Fig. 19.** Ramps optimization plots.**Table 4**  
Published adsorption capacities of biosorbents.

Adsorbent	Adsorption capacity (mg/g)	Refs.
Pine wood char (fast pyrolysis)	4.6	Mohan et al. [32]
Oak wood char (fast pyrolysis)	5.7	Mohan et al. [32]
Meranti sawdust	34.2	Rafatullah et al. [41]
Natural diatomite	25.01	Irani et al. [23]
Tamarind wood (ZnCl <sub>2</sub> activated)	43.9	Acharya et al. [1]
Saw dust	116	Sreejalekshmi et al. [44]
<i>Pinus merkusii</i> (citric acid modified)	82.6	Low et al. [29]
Oil bean shell	1.23	Abugu et al. [6]
<i>African canarium</i>	8.08 (from industrial waste)	Abugu et al. [5]
<i>Terminalia Mantaly</i> seed husk	TM - 93.6TMTM - 99.95NaMTM - 93.60AMTM - 88.2	This study

in the process as was noted by Kul and Caliskan, [26] and Mrozik et al [33]. The adsorption capacities of the biosorbents (Table 2) were higher at higher adsorbate concentration.

Table 4 presents the comparison of the previously reported maximum adsorption capacity of different biosorbents with the prepared adsorbent from *Terminalia mantaly* seed husk toward Pb(II) (at equilibrium). The adsorption capacity of TM, TMTM, NaMTM and, AMTM were relatively higher than most of the listed adsorbents. Beside, the simple, mild conditions and, cost-effective process of TM and TM modified adsorbent preparation transcend the application foreground.

#### Experimental design predictions

In the quest to determine the best adsorbent, the nature of the factors interact and how the percentage of adsorption is dependent on the type and concentration of different adsorbents, an optimal design method (response surface custom method) was used to design this experiment. The different adsorbents compared in this design were TM, TMTM, AMTM and, NaMTM with concentrations of 200, 400, 800 and 1000 mg for each, which gave a design of 16 runs. The design responses were generated for these runs in percentages, and on analyzing these results, model plots and solutions were generated (Fig. 17).

#### ANOVA 2FI model

##### Response 1: percent

The ANOVA (Table 5) showed that the p-value of the two factor interaction model (2FI) is less than 0.005, indicating that it is a good model for the data and for predicting outcomes within the experimental space (200–1000 mg). The ramps optimization plots (Fig. 19) predicted that out of six possible solutions of achieving maximum adsorption, that 1000 mg of TMTM is more desirable (Fig. 18). The model/equation in coded factors is ( $Y$ ) = 94.72 - 3.07A + 1.61 B[1] + 5.21 B[2] - 5.04 B[3] + 0.5050 AB[1] + 3.11 AB[2] - 0.2290 AB[3]

**Table 5**  
Two-factor interaction (2FI) ANOVA model response result.

source	Sum of squares	df	Mean square	F-value	p-value	
<b>Model</b>	381.07	7	54.44	19.94	0.0002	significant
A-con	94.43	1	94.59	34.59	0.0004	
B-adsorbent	233.12	3	77.71	28.47	0.0001	
AB	53.51	3	17.84	6.53	0.0152	
<b>Residual</b>	21.84	8	2.73			
<b>Cor Total</b>	402.91	15				

## Conclusion

A novel *Terminalia mantaly* based adsorbent was prepared by acid, base and thermal modification processes. The morphological characteristics and compositions showed that *Terminalia mantaly* seed husk is a promising source of high-quality biosorbent having possessed higher adsorption capacity than some existing adsorbents. The process of adsorption of Pb<sup>2+</sup> onto TM and TMTM, were very well delineated by pseudo-second-order and Freundlich isotherm models, suggesting that the adsorption of Pb<sup>2+</sup> onto TM and TMTM were pacified by chemosorption, as a result of heterogeneous surface energies which gives an exponential distribution of active sites existing in the adsorbent. This was also predicted by Dubinin Radushkevich isotherm model, suggesting chemosorption. For AMTM and NaMTM, they were delineated by pseudo-second-order and Temkin isotherm models showing that all molecules in the layer of adsorbent decreased linearly rather than logarithmic with coverage due to adsorbent-adsorbate interactions and that the adsorption was characterized by a uniform distribution of the binding energies, up to some maximum binding energy. The TGA also indicated high thermal stability of the precursor as a potential adsorbent for Pb(II) removal from aqueous medium. TMTM was experimentally the best adsorbent having the highest adsorption capacity (99.95 mg/g) as was predicted by the experimental design result.

## Funding

This work was not funded.

## Declaration of Competing Interest

There are no conflicts of interest and no other source of funding except the authors.

## References

- [1] J. Acharya, J.N. Sahu, C.R. Mohanty, B.C. Meikap, Removal of lead (II) from wastewater by activated carbon developed from tamarind wood by zinc chloride activation, *Chem. Eng. J.* 149 (2009) 249–262.
- [2] M. Al Bahri, L. Calvo, M.A. Gilarranz, J.J. Rodriguez, Activated carbon from grape seeds upon chemical activation with phosphoric acid: application to the adsorption of diuron from water, *Chem. Eng. J.* 203 (2012) 348–356, doi:[10.1016/j.cej.2012.07.053](https://doi.org/10.1016/j.cej.2012.07.053).
- [3] B. Acevedo, C. Barriocanal, Texture and surface chemistry of activated carbons obtained from tyre waste, *Fuel Process. Technol.* 134 (2015) 275–283.
- [4] E. Atanes, A. Nieto-Máquez, A. Cambra, M.C. Ruiz-Pérez, F. Fernández-Martínez, Adsorption of SO<sub>2</sub> onto waste cork powder derived activated carbons, *Chem. Eng. J.* 211–12 (2012) 60–67.
- [5] H.O. Abugu, P.A.C. Okoye, V.I.E. Ajije, P.C. Oforde, Preparation and characterisation of activated carbon from agrowastes peanut seed (African Canarium) and palm kernel shell, *international. J. Innov. Res. Dev.* (3) (2014) 13.
- [6] H.O. Abugu, P.A.C. Okoye, V.I.E. Ajije, P.E. Omukuru, U.C. Umeoboshi, Preparation and characterization of activated carbon produced from oil bean (Ugba or Okpaka) and snail shell, *J. Environ. Anal. Chem.* 2 (6) (2015) 1–17, doi:[10.4172/2380-2391.1000165](https://doi.org/10.4172/2380-2391.1000165).
- [7] I. Ali, M. Asim, T.A. Khan, Low cost adsorbents for the removal of organic pollutants from wastewater, *J. Environ. Manag.* 113 (2012) 170–183, doi:[10.1016/j.jenvman.2012.08.028](https://doi.org/10.1016/j.jenvman.2012.08.028).
- [8] C. Aharoni, M. Ungarish, *Kinetics of activated chemosorption, part 2. Theoretical models*, *J. Chem. Soc. Faraday Trans.* 73 (1977) 456–464.
- [9] A. Bazan, P. Nowicki, P. Połrolnicki, R. Pietrzak, Thermal analysis of activated carbon obtained from residue after supercritical extraction of hops, *J. Therm. Anal. Calorim.* 125 (2016) 1199–1204, doi:[10.1007/s10973-016-5419-5](https://doi.org/10.1007/s10973-016-5419-5).
- [10] V.D.A. Cardoso, A.G.D. Souza, P.P.C. Sartoratto, L.M. Nunes, The ionic exchange process of cobalt, nickel and copper(II) in alkaline and acid-layered titanates. *Colloides and surface A, Physicochem. Eng. Aspects* 248 (2004) 145–149.
- [11] F.A. Dawodu, K.G. Akpomie, Simultaneous adsorption of Ni(II) and Mn(II) ions from aqueous solution unto a Nigerian kaolinite clay, *J. Mater. Res. Technol.* 3 (2) (2014) 129–141.
- [12] A. Dabrowski, *Adsorption - from theory to practice*, *Adv. Colloid Interface Sci.* 93 (2001) 135–224.
- [13] J.O. Esalah, M.E. Weber, J.H. Vera, Removal of lead, cadmium and zinc from aqueous solutions by precipitation with sodium di-(n-octyl) phosphinate, *Can. J. Chem.* 78 (2000) 948–954.
- [14] S.I. Eze, H.O. Abugu, L.C. Ekowo, Thermal and chemical pretreatment of cassia sieberiana seed as biosorbent for Pb<sup>2+</sup> removal from aqueous solution, *Desalin. Water Treat.* 226 (2021) 223–241 2021, doi:[10.5004/dwt.2021.27234](https://doi.org/10.5004/dwt.2021.27234).
- [15] T. Fan, Y. Liu, B. Feng, G. Zeng, C. Yang, M. Zhou, H. Zhou, Z. Tan, X. Wang, Biosorption of cadmium(II), zinc(II) and lead(II) by penicillium simplicissimum: isotherms, kinetics and thermodynamics, *J. Hazard. Mater.* 160 (2–3) (2008) 655–661, doi:[10.1016/j.jhazmat.2008.03.038](https://doi.org/10.1016/j.jhazmat.2008.03.038).
- [16] D.P. Facchi, A.L. Cazetta, E.A. Canesin, V.C. Almeida, E.G. Bonafe, M.J. Kipper, A.F. Martins, New magnetic chitosan-alginate-Fe<sub>3</sub>O<sub>4</sub>@SiO<sub>2</sub> hydrogel composites applied for removal of Pb(II) ions from aqueous systems, *Chem. Eng. J.* 337 (2018) 595–608.
- [17] K.Y. Foo, B.H. Hameed, Preparation and characterization of activated carbon from pistachio nut shells via microwave-induced chemical activation, *Biomass Bioenergy* 35 (2011) 3257–3261.
- [18] A. Gunay, E. Arslankaya, I. Tosun, Lead removal from aqueous solution by natural and pretreated clinoptilolite: adsorption equilibrium and kinetics, *J. Hazard. Mater.* 146 (2007) 362–371.

- [19] H.A. Aziz, M.S. Yusoff, M.N. Adlan, N.H. Adnan, S. Alias, Physico-chemical removal of iron from semi-aerobic landfill leachate by limestone filter, *Waste Management & Research* 22 (2004) 371–375.
- [20] O. Hamdaoui, E. Neffrechoux, Modeling of adsorption isotherms of phenol and chlorophenols onto granular activated carbon part I. Two-parameter models and equations allowing determination of thermodynamic parameters, *J. Hazard. Mater.* 147 (2007) 381–394.
- [21] M. Hofman, R. Pietrzak, Adsorbents obtained from waste tires for NO<sub>2</sub> removal under dry conditions at room temperature, *Chem. Eng. J.* 170 (2011) 202–208.
- [22] N.D. Hutson, R.T. Yang, Theoretical basis for the Dubinin-Radushkevitch (D-R) adsorption isotherm equation, *Adsorption* 3 (3) (1997) 189–195.
- [23] M. Irani, M. Amjadi, M.A. Mousavian, Comparative study of lead sorption onto natural perlite, dolomite and diatomite, *Chem. Eng. J.* 178 (2011) 317–323.
- [24] J.N. Nsami, J.K. Mbadcam, The adsorption efficiency of chemically prepared activated carbon from cola nut shells by ZnCl<sub>2</sub> on methylene blue, *J. Chem.* (2013) 2013, doi:[10.1155/2013/469170](https://doi.org/10.1155/2013/469170).
- [25] A.R. Khan, H. Tahir, F. Uddin, H. Uzma, Adsorption of methylene blue from aqueous solution on the surface of wool fiber and cotton fiber, *J. Appl. Sci. Environ. Manag.* 9 (2) (2005) 29–35.
- [26] A.R. Kul, N. Caliskan, Equilibrium and kinetic studies of the adsorption of Zn(II) ions onto natural and activated kaolinites, *Adsorpt. Sci. Technol.* 27 (1) (2009) 85–105.
- [27] R. Levin, M.J. Brown, M.E. Kashtock, D.E. Jacobs, E.A. Whelan, J. Rodman, M.R. Schock, A. Padilla, T. Sinks, Lead exposures in U.S. children, 2008: implications for prevention, *Environ. Health Perspect.* 116 (2008) 1285–1293.
- [28] J. Li, L. Xiao, S. Zheng, Y. Zhang, M. Luo, C. Tong, H. Xu, Y. Tan, J. Liu, O. Wang, F. Liu, A new insight into the strategy for methane production affected by conductive carbon cloth in wetland soil: beneficial to acetoclastic methanogenesis instead of CO<sub>2</sub> reduction, *Sci. Total Environ.* 643 (2018) 1024–1030.
- [29] K.S. Low, C.K. Lee, S.M. Mak, Sorption of copper and lead by citric acid modified wood, *Wood Sci. Technol.* 38 (2004) 629–640.
- [30] B. McEnaney, T.J. Mays, *Introduction to Carbon Science*, Butterworths, London, 1989.
- [31] Y. Wen, Y. Ji, S. Zhang, J. Zhang, G. Cai, A simple low-cost method to prepare lignocellulosic-based composites for efficient removal of Cd(II) from wastewater, *Polymers* 11 (2019) 711 2019, doi:[10.3390/polym111940711](https://doi.org/10.3390/polym111940711).
- [32] D. Mohan, C.U. Pittman, M. Brücke, F. Smith, B. Yancey, J. Mohammad, P.H. Steele, M.F. Alexandre-Franco, V. Gómez-Serrano, H. Gong, Sorption of arsenic, cadmium, and lead by chars produced from fast pyrolysis of wood and bark during bio-oil production, *J. Colloid Interface Sci.* 310 (2007) 57–73.
- [33] W. Mrozik, C. Jungnickel, M. Skup, P. Urbaszek, P. Stepnowski, Determination of the adsorption mechanism of imidazolium-type ionic liquids onto kaolinite: implications for their fate and transport in the soil environment, *Environ. Chem.* 5 (4) (2008) 299–306, doi:[10.1071/EN08015](https://doi.org/10.1071/EN08015).
- [34] S. Mustapha, D.T. Shuaib, M.M. Ndamitso, M.B. Etsuyankpa, A. Sumaila, U.M. Mohammed, M.B. Nasirudeen, Adsorption isotherm, kinetic and thermodynamic studies for the removal of Pb(II), Cd(II), Zn(II) and Cu(II) ions from aqueous solutions using albizia lebbeck pods, *Appl. Water Sci.* 9 (2019) 142, doi:[10.1007/s13201-019-1021-x](https://doi.org/10.1007/s13201-019-1021-x).
- [35] B.Y. Nale, J.A. Kagbu, A. Uzairu, E.T. Nwankwere, S. Saidu, H. Musa, Kinetic and equilibrium studies of the adsorption of lead (II) and Nickel(II) ions from aqueous solutions on activated carbon prepared from maize cob, *Pelagia Res. Libr.* 3 (2) (2012) 302–312.
- [36] P. Nowicki, H. Wachowska, R. Pietrzak, Active carbons prepared by chemical activation of plum stones and their application in removal of NO<sub>2</sub>, *J. Hazard. Mater.* 181 (2010) 1088–1094.
- [37] P. Nowicki, P. Skibiszewska, R. Pietrzak, Hydrogen sulphide removal on carbonaceous adsorbents prepared from coffee industry waste materials, *Chem. Eng. J.* 248 (2014) 208–215.
- [38] A.S. Ozcan, B. Erdem, A. Ozcan, Adsorption of acid blue 193 from aqueous solutions onto na-bentonite and DTMA-bentonite, *J. Colloid Interface Sci.* 280 (1) (2004) 44–54, doi:[10.1016/j.jcis.2004.07.035](https://doi.org/10.1016/j.jcis.2004.07.035).
- [39] G.F. Oliveira, R.C. Andrade, M.A.G. Trindade, H.M.C. Andrade, C.T. Carvalho, Thermogravimetric and spectroscopic study (TG-DTA/FTIR) of activated carbon from the renewable biomass source babassu, *Quím. Nova* 40 (3) (2017) 284–292, doi:[10.21577/0100-4042.20160191](https://doi.org/10.21577/0100-4042.20160191).
- [40] P. Patnukao, P. Pavasant, Activated carbon from Eucalyptus camaldulensis Dehn bark using phosphoric acid activation, *Bioresour. Technol.* 99 (17) (2008) 8540–8543, doi:[10.1016/j.biortech.2006.10.049](https://doi.org/10.1016/j.biortech.2006.10.049).
- [41] M. Rafatullah, O. Sulaiman, R. Hashim, A. Ahmad, Adsorption of copper (II), chromium (III), nickel (II) and lead (II) ions from aqueous solutions by meranti sawdust, *J. Hazard. Mater.* 170 (2009) 969–977.
- [42] A. Sharma, S.A. Chaudhry, Adsorption of pharmaceutical pollutants using lignocellulosic materials, *Environ. Chem. Sustain. World* 38 (2020), doi:[10.1007/978-3-030-17724-9\\_12](https://doi.org/10.1007/978-3-030-17724-9_12).
- [43] S. Shahkarami, R. Azargohar, A.K. Dalai, J. Soltan, Breakthrough CO<sub>2</sub> adsorption in bio-based activated carbons, *J. Environ. Sci.* 34 (2015) 68–76.
- [44] K.G. Sreejalekshmi, K.A. Krishnan, T.S. Anirudhan, Adsorption of Pb(II) and Pb(II)-citric acid on sawdust activated carbon: Kinetic and equilibrium isotherm studies, *J. Hazard. Mater.* 161 (2009) 1506–1513.
- [45] H. Teng, T.S. Yeh, L.Y. Hsu, Preparation of activated carbon from bituminous coal with phosphoric acid activation, *Carbon* 36 (9) (1998) 1387–1395, doi:[10.1016/S0008-6223\(98\)00127-4](https://doi.org/10.1016/S0008-6223(98)00127-4).
- [46] H. Teng, L.Y. Hsu, High-porosity carbons prepared from bituminous coal with potassium hydroxide activation, *Ind. Eng. Chem. Res.* 38 (8) (1999) 2947–2953, doi:[10.1021/ie990101+](https://doi.org/10.1021/ie990101+).
- [47] A. Tomczyk, Z. Sokołowska, P. Boguta, Biochar physicochemical properties: pyrolysis temperature and feedstock kind effects, *Rev. Environ. Sci. Biotechnol.* 19 (2020) 191–215 2020, doi:[10.1007/s11157-020-09523-3](https://doi.org/10.1007/s11157-020-09523-3).
- [48] M. Temkin, V. Pyzhev, Kinetics of Ammonia Synthesis on Promoted Iron Catalysts, *Acta Physicochimica URSS* 12 (1940) 217–222.
- [49] M.T. Uddin, M.S. Islam, M.Z. Abedin, Adsorption of phenol from aqueous solution by water hyacinth ash, *ARPN J. Eng. Appl. Sci.* 2 (2) (2007) 121–128.
- [50] O.C. Ugwoke, B. Dauda, J.A. Ezugwu, H.O. Abugu, L.O. Alum, S.I. Eze, O.A. Odewole, Chromium Adsorption Using Modified Locust Bean and Maize Husk, *Der Pharma Chemica* 12 (5) (2020) 7–14.
- [51] Y.X. Wang, H.H. Ngo, W.S. Guo, Preparation of a specific bamboo based activated carbon and its application for ciprofloxacin removal, *Sci. Total Environ.* 533 (2015) 32–39.
- [52] D.B. Weirich, R. Hari, H. Xue, P. Behra, L. Sigg, Adsorption of Cu, Cd, and Ni on goethite in the presence of natural groundwater ligands, *Environ. Technol.* 36 (2002) 328–336.
- [53] G. Xu, L. Wang, Y. Xie, M. Tao, W. Zhang, Highly selective and efficient adsorption of Hg<sup>2+</sup> by a recyclable aminophosphonic acid functionalized polyacrylonitrile fiber, *J. Hazard. Mater.* 344 (2018) 679–688.
- [54] L. Xia, Z. Huang, L. Zhong, F. Xie, C.Y. Tang, C.P. Tsui, Bagasse cellulose grafted with an amino-terminated hyperbranched polymer for the removal of Cr(VI) from aqueous solution, *Polymer* 10 (2018) 391–405.
- [55] J. Zawadzki, *Chemistry and Physics of Carbon*, Marcel Dekker, Inc., New York, 1989, pp. 79–88. Vol. 21.
- [56] N. Zhang, G.L. Zang, C. Shi, H.Q. Yu, G.P. Sheng, A novel adsorbent TEMPO-mediated oxidized cellulose nanofibrils modified with PEI: preparation, characterization, and application for Cu(II) removal, *J. Hazard. Mater.* 316 (3) (2016) 11–18.
- [57] J. Zheng, Q. Zhao, Z. Ye, Preparation and characterization of activated carbon fibre (ACF) from cotton woven waste, *Appl. Surf. Sci. J.* 299 (2014) 86–91.